Optimal Beam Partitioning and Scheduling for SWIPT Networks

Biagio Boi
dept. of Computer Science
University of Salerno
Fisciano, Italy
bboi@unisa.it

Christian Esposito
dept. of Computer Science
University of Salerno
Fisciano, Italy
esposito@unisa.it

Gustavo de Veciana
dept. of Electrical Engineering
University of Texas at Austin
Austin, USA
deveciana@utexas.edu

***Abstract*—Simultaneous Wireless Information and Power Transfer (SWIPT) enables IoT devices to harvest energy and exchange data over the same wireless infrastructure. In directional SWIPT networks, beam design induces a trade-off between concentrating power on a few users versus broadening energy the harvesting opportunities to a wider set of devices, especially under harvest-then-transmit operation.**

This paper proposes a framework to optimize user-beam association and scheduling of transmission and energy harvesting. As a concrete instantiation, we consider a SWIPT network with directional beams and formulate the corresponding proportional-fair beam design problem under a constraint on the number of active beams. We develop an exact dynamic-programming algorithm that computes the globally optimal non-overlapping beam partition, and we derive an instance-wise upper bound on the loss induced by the non-overlapping restriction under beam-independent scheduling.

Numerical results show that the proposed solution closely tracks this benchmark over a broad range of SWIPT regimes, while highlighting the role of heterogeneity in user distance, density, spatial concentration, and scheduling choices. These findings indicate that non-overlapping beam designs can provide near-optimal performance with a tractable optimization structure.

***Index Terms*—SWIPT, beamforming, dynamic programming, resource allocation.**

I. Introduction

The use of Energy Harvesting (EH) technologies has increased the number of applications for the IoT. The capabilities of EH sources can vary depending on the physical condition of the surrounding environment, such as the availability of solar, thermal, or Radio Frequency (RF) sources. The benefit of RF is that, unlike the other ones, it can be controlled. Among the abovementioned energy harvesting techniques, Simultaneous Wireless Information and Power Transfer (SWIPT) is particularly interesting because it reuses the same architecture for accomplishing data and energy transmission, reducing the space requirements on the IoT device. Existing cellular networks, currently implementing 5G and 6G paradigms, are speeding up the data transmission rates of devices, but can also be leveraged by EH-devices to speed-up their harvesting process. An interesting technique used in those networks is beamforming. Beamforming in traditional networks is known to improve the SINR for selected User Equipment (UE), depending on the beam width. Narrow beams achieve higher SINR as compared to wider beams, although at the cost of reduced coverage. While this trade-off is well studied in communication-centric scenarios, its role in power-based networks remains less understood. In fact, the dynamics underlying power harvesting are qualitatively different from those of information decoding, especially when non-linear EH models are considered. In particular, the presence of sensitivity and saturation thresholds can create regimes where increasing received power yields diminishing returns, whereas the effect of increasing harvesting opportunities (time and exposure to transmissions) may dominate. This creates a scenario where narrowing the beam might not be beneficial, as it reduces the number of users that can harvest energy and increases the risk of missing users due to mobility or imperfect alignment.

A. Related Work

In SWIPT networks, beam design has been investigated in conjunction with user scheduling, spatial switching, and resource allocation, targeting objectives such as energy efficiency [1], fairness, or joint communication–energy performance [2]. A common theme is that directionality can enhance instantaneous received power at selected devices, which is beneficial for both decoding and energy harvesting. Perhaps, the most interesting results are related to the strategic selection of beamforming based on the position of end-devices [1], [3]–[5]. In fact, the RF signal can be passively harvested in SWIPT networks when a Base Station (BS) is transmitting to another user in the same beam [3], [6], especially in the vehicular context [4], [5].

However, two limitations emerge in the existing literature. First, many formulations models the coupling between the downlink energy-transfer process and the uplink transmission of information, i.e., *harvest-then-transmit* protocols [7], [8], but none of them evaluates this in the context of beamforming. Second, non-linear EH behavior (sensitivity and saturation) is often not considered nor integrated into beam scheduling decisions, even though it can qualitatively change the optimality of narrow-beam strategies [9], [10]: beyond saturation, increasing received power yields diminishing returns, whereas increasing harvesting opportunity (time and exposure to transmissions) may dominate. This creates a scenario where narrowing the beam might not be beneficial.

B. Our Contribution

In this paper, we adopt a new perspective on wireless resource allocation. Although SWIPT with directional transmission is the motivating use case, the main contribution is a dynamic-programming framework for a broad class of wireless optimization problems in which service decisions induce a partition of an ordered set of users into contiguous groups. From this viewpoint, beamforming is one possible instantiation of a more general combinatorial structure. Other

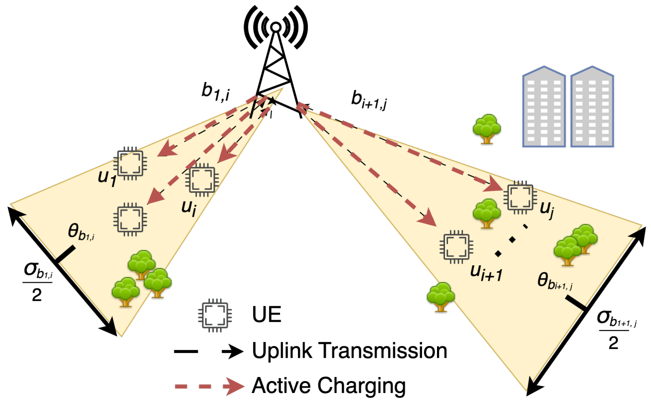

Fig. 1. SWIPT Architecture considered in the system model.

examples of this framework can be the massive cellular networks, where BS might be located close each other.

The contributions of the paper are:

- We identify a class of wireless resource-allocation problems that admit an exact ordered-partition reformulation, and instantiate it on a SWIPT network with directional beams.
- We develop an exact dynamic-programming algorithm that computes the globally optimal non-overlapping beam partition under a proportional-fair objective on rate allocation and a constraint on the number of active beams.
- We characterize the loss induced by the non-overlapping restriction through an instance-wise upper bound under beam-independent scheduling.
- Through numerical evaluations, we show that the proposed DP solution closely tracks this upperbound across a variety of considered SWIPT regimes, and we identify how the gap is affected by user's distance, density, spatial concentration, and the choice of beam-independent scheduler.

The paper is organized into five sections. Section II describes the system model and problem formulation. Section III presents the dynamic programming algorithm for optimal beam partitioning and the analysis of the non-overlapping restriction. Section IV provides numerical results and insights. Finally, Section V concludes the paper and outlines future research directions.

II. System Model and Problem Formulation

We consider a SWIPT network composed of UEs able to harvest RF energy from the downlink transmission of a single BS. The BS uses a set of directional beams, scheduling their activation time over a frame of duration τ. The BS coverage area is modelled as a a disc of radius $r_{\max}$, and each user is located at least a distance $r_{\min}$ from the BS. Each user $u \in \mathcal{U}$ is characterized by a pair $u = (d_u, \kappa_u)$, denoting the distance from the BS and the azimuth, respectively. Users located outside this region are not considered in our model.

Definition 1 (Set of extremal beams $\mathcal{B}$)**.** *We define the set of extremal beams as*

$$\mathcal{B} \triangleq \left\{ b_{i,j}^{(s)} : s \in \{1, \ldots, |\mathcal{U}|\},\ 1 \le i \le j \le |\mathcal{U}| \right\},$$

where $b_{i,j}^{(s)} = \left(\sigma_{i,j}^{(s)}, \theta_{i,j}^{(s)}\right)$ is the beam spanning the contiguous block of users, in circular order, from $(s+i-1) \bmod |\mathcal{U}|$ to $(s+j-1) \bmod |\mathcal{U}|$, where $\sigma_{i,j}^{(s)}$ is the angular width of the covered interval and $\theta_{i,j}^{(s)}$ is its midpoint.

TABLE I
Main notation used in the system model and problem formulation.

Symbol	Description
Network and user model	
$\mathcal{U}$	Set of users or UEs in the network.
d_u	Distance between user u and the BS.
κ_u	Azimuth angle of user u.
$r_{\min}$, $r_{\max}$	Minimum and maximum distance from the BS considered in the coverage region.
τ	Duration of one scheduling frame.
Beam model	
$\mathcal{B}$	Set of admissible extremal beams.
$b_{i,j}^{(s)}$	Extremal beam spanning a contiguous block of users in circular order.
σ_b	Angular width of beam b.
θ_b	Midpoint direction of beam b.
$\mathcal{B}_u$	Set of beams whose main lobe covers user u.
z	Side-lobe antenna gain.
$g(b,u)$	Antenna gain of beam b toward user u.
Scheduling and association variables	
$\boldsymbol{A}$	Beam-user association matrix.
δ_u	Downlink energy-transfer time allocated to user u.
γ_u	Uplink transmission time allocated to user u.
τ_b	Total activation time of beam b for energy transfer.
Channel and rate model	
p^{down}	BS downlink transmit power.
p^{up}	UE uplink transmit power.
N_0	Noise power spectral density.
W	System bandwidth.
α	Path-loss exponent.
c_u	Uplink channel capacity of user u.
r_u	Uplink throughput rate achieved by user u.
Energy harvesting model	
$p_{b,u}$	RF power received by user u from beam b.
$h(y)$	Non-linear RF-to-DC energy harvesting function.
$h_{\max}$	Saturation threshold of the EH circuit.
h_s	Sensitivity threshold of the EH circuit.
χ, ι	Parameters shaping the sigmoidal harvesting function.
$h_{b,u}$	Harvested power by user u from beam b.
e_u^{harv}	Total energy harvested by user u.
e_u^{cons}	Energy consumed by user u during uplink transmission.

We assume that the BS can only activate beams in the set of extremal beams $\mathcal{B}$. Lemma 1 shows that this set is sufficient to achieve the optimal performance, and thus the restriction does not cause any loss of optimality. To create the set of all the extremal beams, we consider all possible contiguous blocks of users in circular order.

Depending on the beam configuration and on the spatial distribution of users, a user may lie within the coverage area of one or more main-lobe beams. We let $\mathcal{U}_b \subseteq \mathcal{U}$ denote the set of users covered by the main lobe of beam b, whose cardinality is denoted by $|\mathcal{U}_b|$. Let $\mathcal{B}_u \subseteq \mathcal{B}$, be the subset of beams covering the user u. Since sector coverages may overlap, it generally holds that $\sum_{b\in\mathcal{B}} |\mathcal{U}_b| \ge |\mathcal{U}|$.

A. UE-Beam Association Model

As mentioned earlier, UEs may be covered by multiple active beams, but are always associated (for data transmission purposes) with a single beam. Nevertheless, for energy harvesting purposes it may be beneficial to cover a user with other beams. The adjacency matrix ($\boldsymbol{A}_{bu} : b \in \mathcal{B}, u \in \mathcal{U}$) denotes the data transmission association between beam b and user u (i.e. $\boldsymbol{A}_{bu} = 1$ if beam b is serving uplink service to user u and 0 otherwise). The optimal association strategy is discussed in the next section, where it is formulated as the solution to an optimization problem.

B. Resource Allocation Model

We consider the case where the BS allocates to each user an uplink transmission time γ_u and a downlink service (energy-transfer) time δ_u within a total frame length τ. The following equality must hold for allocation (i.e., no time is left unused):

$$\sum_{u \in \mathcal{U}} (\gamma_u + \delta_u) = \tau. \tag{1}$$

We assume users cannot transmit if they have not harvested enough energy to support the transmissions, and possess an ideal battery[1] for storing the harvested energy needed for transmission. We assume that a user can harvest energy both when scheduled for EH in its allocated time and beam and when the BS is serving other users on a beam that also covers the user. As we will see, the harvested energy of user u depends on the time that the beams covering the user are active for energy transfer. The activation time of a beam b for energy transfer is, in turn, given by:

$$\tau_b = \sum_{u \in \mathcal{U}} \boldsymbol{A}_{bu} \delta_u. \tag{2}$$

C. Channel and Energy Harvesting Model

For analytical tractability, we adopt a classical sectored antenna model [11], which captures the main features relevant to beamforming: directivity gain, half-power beamwidth, and side-lobe leakage. In this model, that will be used in capturing downlink energy harvesting efficiency below, the antenna gain is constant within the main lobe and equal to a reduced constant z in the side lobes. The gain of beam b, towards the user u is:

$$g(b,u) = \begin{cases} \dfrac{2\pi - (2\pi - \sigma_b) z}{\sigma_b}, & |\theta_b - \kappa_u| \leq \frac{\sigma_b}{2}, \\ z, & \text{otherwise}. \end{cases} \tag{3}$$

Meanwhile, we assume the uplink transmission are omni-directional and the transmit power is equal for all of the UEs and is denoted by p^{up}; while the BS transmits at transmit power p^{down}. Thermal noise is modeled as AWGN with power spectral density N_0 W/Hz. The capacity of the uplink channel between user u and the BS is given by

$$c_u = W \log_2 (1 + \frac{p^{\text{up}} d_u^{-\alpha}}{N_0 W}), \tag{4}$$

where W denotes the bandwidth (i.e., UE transmission are omnidirection with path loss α). The uplink throughput rate of user u is then given by:

$$r_u = \frac{\gamma_u c_u}{\tau}. \tag{5}$$

Regarding the harvesting process, the power $p_{b,u}$ received by the user u from the beam b is given by

$$p_{b,u} \ = \ p^{\text{down}} \, g(b,u) \, d_u^{-\alpha}. \tag{6}$$

[1]A time homogeneous inefficiency can be easily introduced.

The efficiency of the harvesting modules is modeled by a non-linear function capturing the characteristics of the RF-to-DC conversion circuitry. We adopt a sigmoidal model [12], which captures both the sensitivity, which is the minimal amount of power to activate the EH circuit, and the saturation, which is the maximum amount of RF power that is possible to harvest:

$$h(y) = \max \left[\frac{h_{\max}}{e^{-\chi h_s + \iota}} \left(\frac{1 + e^{-\chi h_s + \iota}}{1 + e^{-\chi y + \iota}} - 1 \right), 0 \right], \tag{7}$$

where $h_{\max}$ is the saturation threshold, h_s the sensitivity threshold, and χ, ι are shaping parameters. The power harvested by the user u from the beam b is denoted by $h_{b,u} = h(p_{b,u})$. The total amount of harvested energy will be the weighted sum of the beam activation times the power received from each beam. The energy harvested from all the beams covering the user u is thus given by:

$$e_u^{\text{harv}} = \sum_{b \in \mathcal{B}_u} \tau_b \, h_{b,u} \tag{8}$$

while the energy consumed during the uplink transmission is:

$$e_u^{\text{cons}} = \gamma_u \, p^{\text{up}}. \tag{9}$$

For this work, we considered neglegible energy consumption for the downlink phase, as devices does not spend time in downloading data, but uses the whole downlink time for harvesting. We consider a scheduing of users to be feasibile, the uplink and EH time periods are such that the energy harvested is greater than or equal to the energy consumed, i.e., for all $u \in \mathcal{U}$,

$$e_u^{\text{harv}} \geq e_u^{\text{cons}}. \tag{10}$$

Note that users achievable transmission rate is couples together through the energy harvesting process, which depends on the beam design and scheduling decisions.

D. Problem Formulation

Having clarified the system model and taking into account that this work aims to get fundamental insights on the use of beamforming in SWIPT networks, we now formulate the optimization problem that maximizes the logarithmic utility of the rate allocation across users.

Problem 1 (Proportional-Fair Uplink Rate Maximization and Energy Harvesting)**.**

$$\max_{\boldsymbol{A}, \{(\delta_u, \gamma_u)\}_{u \in \mathcal{U}}} \ \sum_{u \in \mathcal{U}} \log\Big(\frac{\gamma_u c_u}{\tau}\Big) \tag{11}$$

$$\textit{s.t.} \quad \tau_b = \sum_{u \in \mathcal{U}} \boldsymbol{A}_{bu} \delta_u, \quad \forall b \in \mathcal{B}; \tag{12}$$

$$\sum_{b \in \mathcal{B}_u} \tau_b \, h_{b,u} \ \geq \gamma_u \, p^{\text{up}}, \ \forall u \in \mathcal{U}; \tag{13}$$

$$\sum_{u \in \mathcal{U}} (\delta_u + \gamma_u) = \tau, \quad \delta, \gamma \geq 0; \tag{14}$$

$$\sum_{b \in \mathcal{B}} \boldsymbol{A}_{bu} = 1, \ \forall u \in \mathcal{U}; \tag{15}$$

$$\boldsymbol{A}_{bu} \in \{0, 1\}, \ \forall u \in \mathcal{U}, \ \forall b \in \mathcal{B}. \tag{16}$$

Here, $\boldsymbol{A} \in \{0,1\}^{|\mathcal{B}| \times |\mathcal{U}|}$ denotes the association matrix between users and beams. Constraint (13) ensures that each user has sufficient harvested energy to support uplink transmission. Constraint (14) enforces the global frame duration, on which scheduling decisions are made. Constraint (15) guarantees that each user is associated with exactly one beam.

Lemma 1 (Sufficiency of extremal beam set $\mathcal{B}$)**.** *Consider any beam $\tilde{b}$ that is not in the set of extremal beams $\mathcal{B}$. Then, there exists an extremal beam $b_{i,j} \in \mathcal{B}$ which achieves a better harvested energy for all users, while covering the same set of users in its main lobe. Hence, there always exists an optimal solution whose beams all belong to the admissible set $\mathcal{B}$.*

Proof. Appendix A. □

Lemma 1 shows that the optimal beamforming design can be restricted to the finite set $\mathcal{B}$ of beams defined by the extremal users in the circular ordering. This is a key structural property that allows us to formulate Problem 1 in terms of the partition of users into contiguous blocks induced by the selected beams.

III. Dynamic Optimization Framework

This section develops a Dynamic-Programming (DP) framework for the considered optimization problem, highlighting the structural conditions that enable an exact ordered-partition solution. The SWIPT system introduced in the previous section is used as a concrete instantiation of this general framework.

A. Dynamic programming formulation

The DP developed in this section is exact for a structured subclass of Problem 1. In particular, it relies on two conditions: a geometric condition on the beam configuration and a scheduling condition on the service times allocated to the users.

Assumption 1 (Non-overlapping beams)**.** *The active beams in a feasible solution are non-overlapping in the angular domain.*

Assumption 2 (Beam independent scheduling policy)**.** *A scheduling policy is said to be a beam independent policy if it assigns to each user $u \in \mathcal{U}$ a service budget $t_u > 0$, independently of the beam assignment, such that*

$$\sum_{u \in \mathcal{U}} t_u = \tau.$$

Typical examples of beam-independent scheduling policy include equal-time allocation across beams, fixed per-beam resource budgets, and predetermined local rules in which the resource assigned to a beam depends only on its own attributes (e.g., beamwidth or number of covered UEs), but not on the set of other scheduled beams. By contrast, jointly optimized allocations under a global coupling constraint, such as $\sum_k t_k \leq T$, do not satisfy this assumption.

Assumption 1 implies that, once the UEs are ordered by azimuth angle, the users served by the same beam form a contiguous interval in the ordering. Assumption 2 implies that the dedicated time for each users uplink transmission and downlink energy harvesting, e.g. $t_u = \gamma_u + \delta_u$, is independant of the choice of beams used to serve the users. Therefore, under Assumption 1 and Assumption 2, the global objective and feasibility constraints decompose across intervals, and Problem 1 can be reduced to an ordered-partition problem.

Let $N \triangleq |\mathcal{U}|$, index UEs in increasing azimuth order as $1, 2, \ldots, N$, and let K be the maximum number of beams to be scheduled. As depicted in Fig. 2, we linearize the circular order by choosing a starting UE index $s \in \{1, \ldots, N\}$ and considering the sequence $s,\ s+1,\ \ldots,\ s+N-1 \pmod N$.

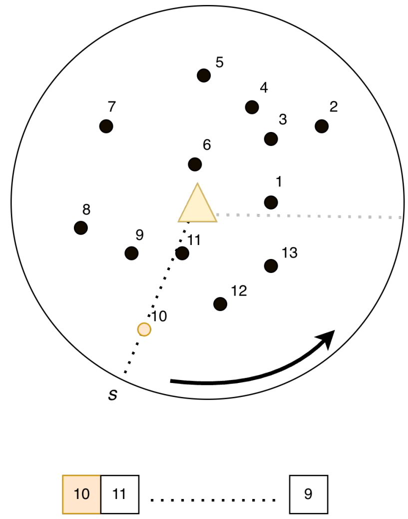

Fig. 2. Linearization of the circular UE order. UEs are randomly located inside the disc, but indexed according to their azimuth with respect to the BS. Once the starting index s is selected, the circular order is unrolled into the sequence $s, s+1, \ldots, s+N-1 \pmod N$.

An interval of UEs $i, \ldots, j \pmod N$ is served by the beam covering the corresponding angular interval, with boresight at its midpoint. We define the interval value $w_s(i,j)$ as the maximum proportional-fair utility achievable by that interval:

$$\begin{aligned} w_s(i,j) \triangleq &\max_{\{(\delta_u,\gamma_u)\}_{u=i}^{j}} \sum_{u=i}^{j} \log(\gamma_u) && \text{(17a)}\\ \text{s.t.}\quad & \delta_u + \gamma_u = t_u, \quad u = i, \ldots, j, && \text{(17b)}\\ & \gamma_u\, p^{\mathrm{up}} \leq h_{b_{i,j},u} \sum_{r=i}^{j} \delta_r, \quad u = i, \ldots, j, && \text{(17c)}\\ & \delta_u \geq 0,\ \gamma_u \geq 0, \quad u = i, \ldots, j. && \text{(17d)} \end{aligned}$$

where $h_{b_{i,j},u}$ is the harvested power experienced by user u when served by beam $b_{i,j}$. If no feasible allocation exists for interval $[i,j]$, then $w_s(i,j) = -\infty$. The key observation enabling a DP-based solution is that, according to Assumption 2, the interval value $w_s(i,j)$ can be optimized locally, independently of how the remaining users are grouped, provided that each user's service budget t_u is determined prior to beam allocation. The total objective is, therefore, the sum of interval values. Hence, the optimization over beam boundaries and the optimization of time allocations within each interval decouple, and the global problem reduces to that of selecting the partition into at most K contiguous intervals which maximize the sum of interval values:

$$W_s^\star = \max_{\substack{m \in \{1,\ldots,K\} \\ 1 \leq j_1 < \cdots < j_m = N}} \left\{ w_s(1, j_1) + \sum_{q=2}^{m} w_s(j_{q-1}+1, j_q) \right\}. \tag{18}$$

B. Algorithm

Direct enumeration of (18) is combinatorial: for a fixed m, there are $\binom{N-1}{m-1}$ partitions, and the search space grows exponentially in N. We overcome this via dynamic programming by exploiting the optimal substructure of the optimal solution of the problem.

Theorem 1 (Exact DP under non-overlapping beams and beam independent scheduling policies)**.** *Under Assumption 1 and Assumption 2, the restriction of Problem 1 to at most K active beams is equivalent, for each starting index s, to selecting a partition of the linearized user sequence into at most K contiguous non-empty intervals maximizing the sum of their interval values:*

$$W_s^\star = \max_{\substack{m\in\{1,\dots,K\}\\ 1\le j_1<\cdots<j_m=N}} \left\{ w_s(1,j_1) + \sum_{q=2}^{m} w_s(j_{q-1}+1, j_q) \right\}.$$

Moreover, $W_s^\star$ is computed exactly by the recursion

$$F_s(n,1) = w_s(1,n), \tag{19}$$

and, for $2 \le m \le K$ and $m \le n \le N$,

$$F_s(n,m) = \max_{m-1\le j\le n-1} \{F_s(j,m-1) + w_s(j+1,n)\}, \tag{20}$$

with

$$W_s^\star = \max_{1\le m\le K} F_s(N,m).$$

The global optimum is then

$$W^\star = \max_{s\in\{1,\dots,N\}} W_s^\star.$$

Proof. Appendix B. □

C. Complexity

a) Computational complexity: For a fixed starting index s, the DP table $F_s(n,m)$ contains $\mathcal{O}(KN)$ states. For each state with $m \ge 2$, the Bellman update maximizes over at most N candidate cut points, yielding $\mathcal{O}(KN^2)$ candidate split evaluations for that starting position. Repeating the procedure over all N possible starting indices gives $\mathcal{O}(KN^3)$ overall.

In addition, for each fixed s, all $\mathcal{O}(N^2)$ interval values must be precomputed. If each interval value is computed at cost C_w, this requires $\mathcal{O}(N^2C_w)$ operations per starting index, and therefore $\mathcal{O}(N^3C_w)$ overall. Hence, the total computational complexity is $\mathcal{O}\big(N^3(K + C_w)\big)$.

b) Space complexity: For a fixed starting index s, storing the DP table requires $\mathcal{O}(KN)$ memory locations, while storing all precomputed interval values requires $\mathcal{O}(N^2)$ memory locations. Since the N starting indices are processed sequentially, these memory requirements do not accumulate across different values of s. Therefore, the overall space complexity is $\mathcal{O}(KN + N^2)$.

D. Optimality gap under non-overlapping beams

Let $J_{\text{ov}}^\star$ and $J_{\text{no}}^\star$ denote the optimal values of Problem 1 with and without the non-overlapping beam restriction, respectively. Define

$$\bar{h}_u \triangleq \max_{b\in\mathcal{B}} h_{b,u}, \tag{21}$$

i.e., the highest energy harvesting efficiency that user u can achieve over all possible beams. The following result bounds the suboptimality introduced by the non-overlapping restriction through a coupled relaxation that matches the benchmark used in the experiments. To derive a tighter upper bound on $J_{\text{ov}}^\star$, we consider an auxiliary problem that preserves the proportional-fair objective of Problem 1 while replacing the original beam-assignment and harvesting constraints with a coupled outer relaxation expressed only in terms of (γ, T).

Lemma 2 (Optimality gap under beam-independent scheduling)**.** *Fix an instance $\mathcal{I}$ and a beam-independent scheduling policy π that assigns user service budgets $\{t_u\}_{u\in\mathcal{U}}$, with $t_u > 0$ for all $u \in \mathcal{U}$ and $\sum_{u\in\mathcal{U}} t_u = \tau$. Let $J_{\text{ov}}^\star$ and $J_{\text{no}}^\star$ denote the optimal values of Problem 1 for instance $\mathcal{I}$ and policy π with and without the non-overlapping beam restriction, respectively. Let γ_u^{DP} denote the uplink time of user u under the optimal non-overlapping DP solution, and let $(\hat{\gamma}, \hat{T})$ be an optimizer of*

$$\max_{\gamma,T} \sum_{u\in\mathcal{U}} \log\left(\frac{\gamma_u c_u}{\tau}\right) \tag{22}$$

subject to

$$0 \le \gamma_u \le t_u, \qquad \forall u \in \mathcal{U}, \tag{23}$$

$$\gamma_u p^{\text{up}} \le \bar{h}_u T, \qquad \forall u \in \mathcal{U}, \tag{24}$$

$$T + \sum_{u\in\mathcal{U}} \gamma_u = \tau, \qquad T \ge 0. \tag{25}$$

Then

$$0 \le J_{\text{ov}}^\star - J_{\text{no}}^\star \le \sum_{u\in\mathcal{U}} \log\left(\frac{\hat{\gamma}_u}{\gamma_u^{\text{DP}}}\right). \tag{26}$$

In particular, if $\gamma_u^{\text{DP}} = \hat{\gamma}_u, \forall u \in \mathcal{U}$, then $J_{\text{no}}^\star = J_{\text{ov}}^\star$.

Proof. Appendix C. □

IV. Experimental Results

Having defined the system model and the dynamic programming framework, we now present a set of preliminary results. The aim of this section is to provide insights into the system performance under different configurations. In particular, we focus on the impact of key parameters such as the maximum user distance from the BS ($r_{\max}$), the user density (λ_u), and the users' spatial distribution on the optimal beamforming strategy, as well as on the resulting throughput and energy harvesting performance.

A. Setup

To conduct the experiments, we considered a scenario with a single BS capable of performing beamforming through IRS support. The BS covers a variable area with $r_{\min} = 2$ meters and $r_{\max}$ ranging from 10 to 60 meters, while the UE spatial density λ_u varies from 2×10^{-3} to 10×10^{-3}, unless otherwise specified. The users might be distributed in one or more clusters. In the experiments we mostly refer to clusters of 40 degrees for UE distribution, representing a good trade-off between narrowness and wide distribution. BS delivers energy over the NB-IoT channel, operating with a bandwidth of 180 kHz. For the path-loss model, we adopted $\alpha = 3.5$, which is commonly used to represent suburban macrocell scenarios with moderate propagation losses. The frame duration τ is normalized to 1. The downlink transmission power p^{down} is set to 4 W, with the radiated power adjusted according to the beam directionality.

We next assess the proposed DP formulation against a heuristic that iteratively places fixed 10-degree beams centered on the uncovered user with the lowest received power, serving as a simple baseline for comparison. For each realization, the scheduler assigns a fixed service budget $t_u > 0$ to every user u, independently of the beam assignment, with $\sum_{u\in\mathcal{U}} t_u = \tau$. We considered three service policies are: i) TDMA Equal Service Time scheduling, with $t_u = \tau/|\mathcal{U}|$; ii) TDMA Inverse-Distance Weighted Service Time, with budgets inversely proportional to r_u; and iii) TDMA Distance Weighted Service Time, with budgets proportional to r_u. In all cases, the weights are normalized so that the total allocated service time matches the frame duration τ.

B. Analysis

Fig. 3 and Fig. 4 compare the mean and minimum per-user throughput achieved by the proposed non-overlapping DP solution with respect to the theoretical upper bound, and to the best-energy heuristic on 10 degrees of aperture as a function of $r_{\max}$, for different angular UE cluster distributions. The only case where the DP solution achieves the upper bound is when users are concentrated in a single cluster and located close to the BS, which is consistent with the intuition that, in this scenario, the optimal beam design consists of a single beam covering all users. In the other cases, a gap emerges as $r_{\max}$ increases, which is more evident when users are distributed across the disk. This is because, as $r_{\max}$ increases, the potential benefits of overlapping beams for users located farther from the BS become more significant, while the non-overlapping constraint limits the ability of the DP solution to exploit these benefits. In these latter scenarios, it is reasonable to expect that overlapping beams may become more beneficial, since they can provide energy to users located farther from the BS, while an additional beam can be used to serve users close to the BS, which are more likely to operate in the saturation regime. Anyway, by looking at the red lines, it is evident that DP achieves very good performance, clearly better than the best-energy heuristic, and only slightly similar when increasing increase $r_{\max}$ and distributing users across the disk, which suggests that non-overlapping beam designs can provide near-optimal performance with a tractable optimization structure. The best-energy heuristic performs very far in all the scenarios, which suggests that, while it can be effective in cases where the context is highly dense, it is not a reliable strategy across different configurations, and thus highlights the importance of optimizing the beam design based on the specific user distribution and system parameters. In fact devices benefit from a wider aperture when they are close to the BS, since they can harvest energy for more time, while they benefit from a narrower beam when they are far from the BS, since they can harvest more energy.

Fig. 5 illustrates the average harvestable energy at the maximum distance $r_{\max}$ as a function of $r_{\max}$ for different beam designs. This figure motivates the finding of Fig. 3 and Fig. 4, since for a single cluster of users, the optimal beam design consists of a single beam covering all users, which yields the highest harvestable energy for users at distance $r_{\max}$. However, as the number of clusters increases, the optimal beam design might consist of a wider beam for closer users (able to harvest more energy despite its narrowness), and an additional beam towards the worst-case users.

The results show that, although narrowing the beam can enhance the harvested energy for users far from the BS, it does not necessarily translate into higher harvested energy for users close to the BS. By jointly considering Fig. 5 and Fig. 3, it is possible to understand the origin of the observed gap between the DP solution and the upper bound. This gap is related to the interplay between beamforming gains and the non-linear characteristics of energy harvesting, which can lead to saturation effects that limit the benefits of narrow

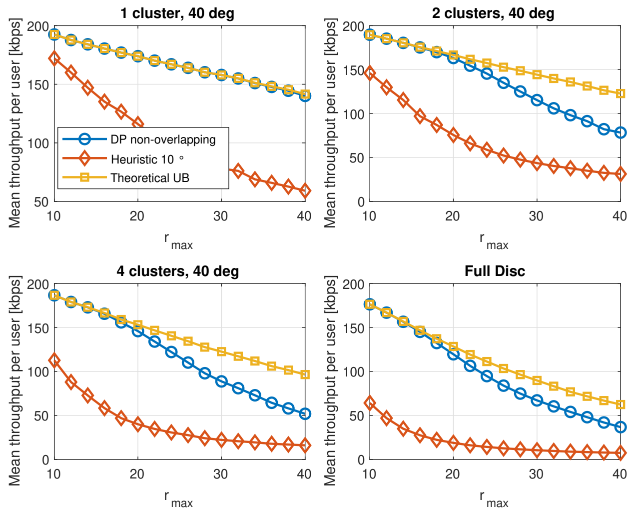

Fig. 3. Maximum UE distance ($r_{\max}$) versus average per-user throughput for different numbers of clusters representing the UE distribution over the disk, comparing the proposed dynamic programming approach with heuristic and the theoretical upper bound.

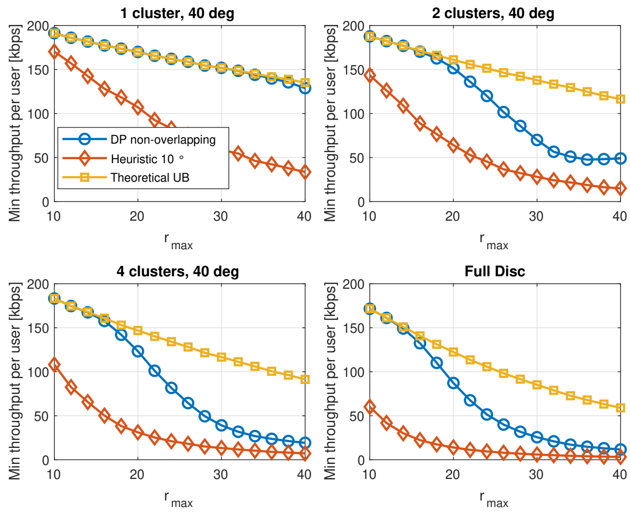

Fig. 4. Maximum UE distance ($r_{\max}$) versus minimum per-user throughput for different numbers of clusters representing the UE distribution over the disk, comparing the proposed dynamic programming approach with heuristic and the theoretical upper bound.

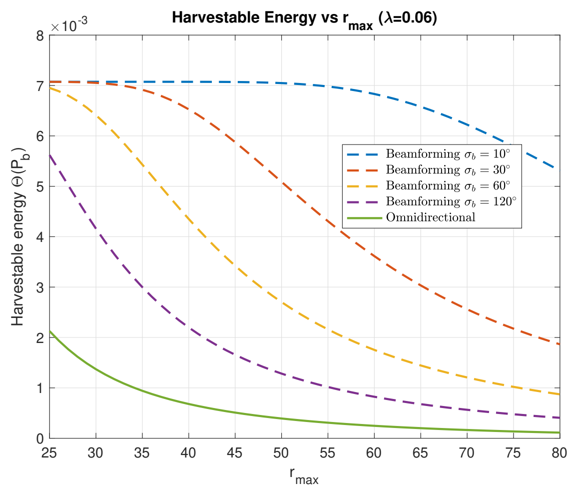

Fig. 5. Harvestable energy at distance $r_{\max}$ versus $r_{\max}$, for $\lambda = 0.06$ and $\sigma_b = \frac{10\pi}{180}$, with different numbers of active beam sectors in the disk.

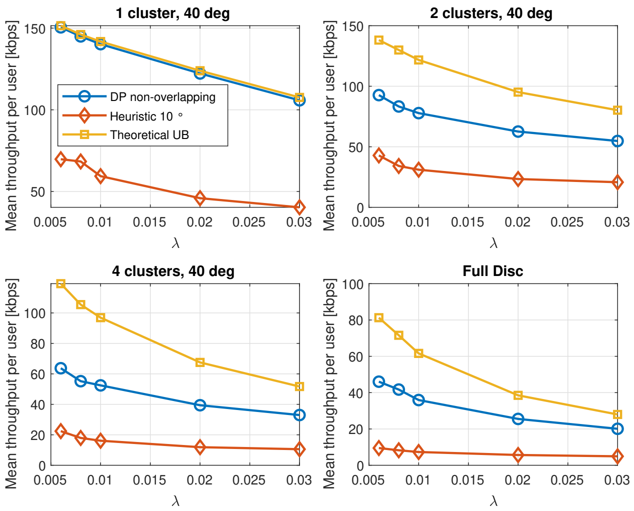

Fig. 6. UE density (λ) versus average per-user throughput for different numbers of clusters representing the UE distribution over the disk, comparing the proposed dynamic programming approach with heuristic and the theoretical upper bound.

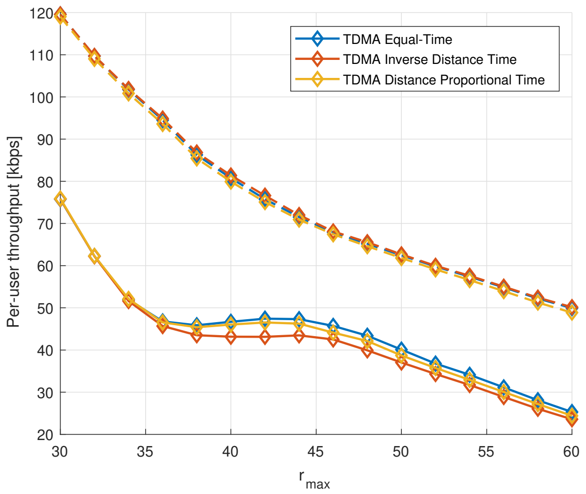

Fig. 7. Minimum (solid line) and average (dashed line) per-user throughput versus $r_{\max}$ for multiple scheduling algorithms, with $\lambda = 0.01$ and 2 clusters of 40 degrees each representing the UE distribution over the disk.

beams for nearby users, thereby reducing the advantage of beam overlapping.

Fig. 6 shows the mean per-user throughput as a function of the user density for different angular UE distributions. As in the previous figure, the DP yields good results when users are distributed within a single cluster. However, in this case, increasing the number of users reduces the gap between the DP solution and the upper bound, even when users are distributed across the disk. This is because, as the density increases, the probability of having users in the saturation regime also increases, which reduces the potential benefits of overlapping beams for users close to the BS and thus narrows the gap between the DP solution and the upper bound.

Figure 7 compares the minimum and average per-user throughput achieved under different beam-independent scheduling policies as a function of $r_{\max}$. As expected, the minimum and average per-user throughput decreases with $r_{\max}$, since enlarging the service region increases both the average user distance and the number of UEs in the area.

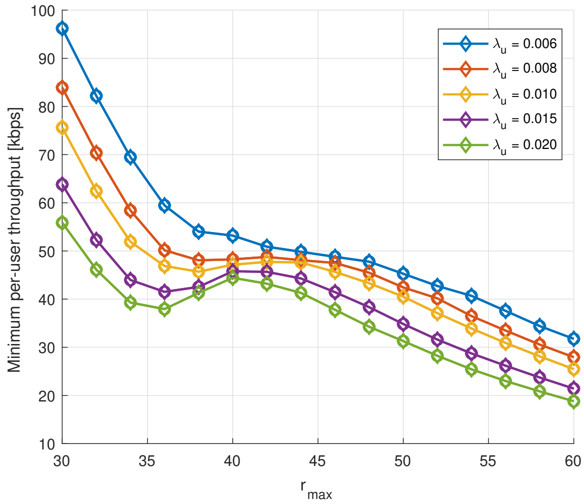

Fig. 8. Minimum per-user throughput versus $r_{\max}$ for equal-time scheduling algorithms, with varying λ and 2 clusters of 40 degrees each representing the UE distribution over the disk.

Regarding the considered scheduling policies yield very similar trends. Among the tested policies, the inverse-distance proportional scheduling consistently yields the worst performance, with a slightly lower throughput, which is consistent with its tendency to allocate more service time to close users. By contrast, equal-time scheduling consistently provides the best performance, since it does not bias the service budget toward users with more budget, which are more likely to operate in the saturation regime.

Anyway, an interesting point is that presence of a flat, nearly increasing region. This region suggests a transition regime in which the loss due to larger distances is partly offset by the larger number of users within each angular cluster. In this regime, additional users increase harvesting opportunities from active beams, which helps sustain the throughput of the weakest users. For larger $r_{\max}$, however, the distance penalty becomes dominant, and the minimum throughput decreases monotonically. This behavior is further analyzed in Fig. 8, where the minimum per-user throughput is plotted as a function of $r_{\max}$ for different user densities under equal-time scheduling. The figure confirms the presence of beneficial regimes between 40 and 50 meters, where the increase in the number of users within each cluster, and thus the presence of additional users in terms of harvesting opportunities become more significant. This corresponds to regimes where the solution picked from the DP has just one beam, and which is going to getting saturated.

V. Conclusion

In this work we investigated the optimal beamforming strategy for a SWIPT network, where a BS equipped with an IRS delivers energy to a set of UEs equipped with energy harvester modules while receiving data from them. We considered a scenario where the location of the devices is known. We demonstrated the optimality of choosing beam patterns based on the user distribution. Additionally, we developed a dynamic programming algorithm to compute the optimal non-overlapping beam partition under a proportional-fair objective and a constraint on the number of active beams. We also derived an instance-wise upper bound on the loss induced by the non-overlapping restriction under beam-independent scheduling. Our results show that the optimal strategy strongly depends on the user distribution, and that omnidirectional transmission can be advantageous in scenarios with high user density and short distances from the BS, while beamforming can be beneficial in scenarios with low user density and long distances from the BS.

Future work will focus on extending the analysis to more complex scenarios, such as multi-cell networks and dynamic user distributions, as well as exploring machine learning techniques for adaptive beamforming design.

APPENDIX

A. Sufficiency of extremal beam set $\mathcal{B}$

Consider any beam $\tilde{b} = (\tilde{\sigma}, \tilde{\theta})$ used in a feasible solution, and let $\mathcal{U}_{\tilde{b}} \subseteq \mathcal{U}$ be the set of users covered by its main lobe. Since the main lobe of a directional beam is a connected angular interval, the users in $\mathcal{U}_{\tilde{b}}$ form a contiguous partition in the circular angular ordering. Let $b_{i,j}^{(s)} \in \mathcal{B}$ be the beam whose angular support is the smallest interval containing those users, i.e., the beam whose boundaries are determined by the two extremal covered users. By construction, $b_{i,j}^{(s)}$ covers exactly the same users as $\tilde{b}$ and has beamwidth $\sigma_{i,j} \leq \tilde{\sigma}$.

Under the adopted sectored antenna model, the main-lobe gain of a beam of width σ is

$$G(\sigma) = \frac{2\pi - (2\pi - \sigma)z}{\sigma} = z + \frac{2\pi(1-z)}{\sigma}.$$

Since $z < 1$, we have $\frac{dG(\sigma)}{d\sigma} = -\frac{2\pi(1-z)}{\sigma^2} < 0$, hence the main-lobe gain is strictly decreasing in the beamwidth.

Therefore, for every user $u \in \mathcal{U}_{\tilde{b}}$, $g(b_{i,j}, u) = G(\sigma_{i,j}) \geq G(\tilde{\sigma}) = g(\tilde{b}, u)$. For every user $u \notin \mathcal{U}_{\tilde{b}}$, both beams keep u outside the main lobe, hence $g(b_{i,j}, u) = g(\tilde{b}, u) = z$. Thus, for all users $u \in \mathcal{U}$, $p_{b_{i,j},u} \geq p_{\tilde{b},u}$. Since the harvesting function $h(\cdot)$ is non-decreasing, it follows that

$$h\big(p_{b_{i,j},u}\big) \geq h\Big(p_{\tilde{b},u}\Big), \qquad \forall u \in \mathcal{U}.$$

Now replace $\tilde{b}$ with $b_{i,j}$ while keeping unchanged the association variables $\boldsymbol{A}$ and the time allocation variables. The beam activation time remains the same, since it depends only on the users associated with that beam through

$$t_b = \sum_{u \in \mathcal{U}} \boldsymbol{A}_{bu} \delta_u.$$

Hence, the harvested energy of every user is strictly increasing. As a consequence, feasibility is preserved, and the objective value of Problem 1 cannot decrease because larger harvested energy can only enlarge the feasible set of uplink times.

Applying this replacement independently to every beam in the solution yields another feasible solution, with objective value no smaller, whose beams all belong to $\mathcal{B}$. Therefore, restricting the search to $\mathcal{B}$ does not affect optimality.

B. Proof of Theorem 1

Fix s and consider the corresponding linearized ordering $i, \ldots, j \pmod N$. Under the non-overlapping beam assumption, any feasible solution partitions this ordered sequence into contiguous non-empty intervals.

Now consider any interval $[i, j]$. Since the service budget of each user is fixed ex ante, the total budget associated with the interval is

$$T_s(i,j) = \sum_{\ell=i}^{j} t_\ell, \tag{27}$$

which depends only on the users belonging to that interval and not on how the remaining users are grouped into other beams. Therefore, once an interval is fixed, its contribution to the objective can be optimized locally, yielding the interval value $w_s(i,j)$.

Because beams are non-overlapping, each user belongs to exactly one interval, and both feasibility and objective contributions separate across intervals. Hence, the value of any partition

$$[1, j_1],\ [j_1+1, j_2],\ \ldots,\ [j_{m-1}+1, j_m], \qquad j_m = N,$$

is exactly

$$w_s(1, j_1) + \sum_{q=2}^{m} w_s(j_{q-1}+1, j_q),$$

which proves (18).

The corresponding DP follows from optimal substructure. If $m = 1$, the only feasible partition of the first n users consists of the single partition $[1, n]$, whose value is $w_s(1, n)$, thus proving (19).

Now consider $m \geq 2$. Any feasible partition of the first n users into m contiguous non-empty partitions has a unique last partition of the form $[j+1, n]$, for some $m-1 \leq j \leq n-1$. The contribution of this partition is equal to the sum of: i) the value of a partition of the first j users into $m-1$ contiguous partitions, and ii) the value $w_s(j+1, n)$ of the last partition. By optimality, the first term is $F_s(j, m-1)$. Therefore, for each admissible j, the best partition ending with partition $[j+1, n]$ has value $F_s(j, m-1) + w_s(j+1, n)$. Maximizing over all admissible j yields (20).

C. Proof of the Gap Bound

For any feasible solution of Problem 1, possibly with overlapping beams, the harvested energy satisfies

$$e_u^{\mathrm{harv}} = \sum_{b \in \mathcal{B}_u} \tau_b\, h_{b,u} \leq \bar{h}_u \sum_{b \in \mathcal{B}} \tau_b.$$

Using (12) and (15),

$$\sum_{b \in \mathcal{B}} \tau_b = \sum_{b \in \mathcal{B}} \sum_{v \in \mathcal{U}} \boldsymbol{A}_{bv} \delta_v = \sum_{v \in \mathcal{U}} \delta_v \sum_{b \in \mathcal{B}} \boldsymbol{A}_{bv} = \sum_{v \in \mathcal{U}} \delta_v.$$

Since π is beam-independent, $\delta_v + \gamma_v = t_v$ for all v, and since $\sum_{v \in \mathcal{U}} t_v = \tau$, it follows that

$$\sum_{b \in \mathcal{B}} \tau_b = \sum_{v \in \mathcal{U}} \delta_v = \sum_{v \in \mathcal{U}} (t_v - \gamma_v) = \tau - \sum_{v \in \mathcal{U}} \gamma_v.$$

Therefore, $e_u^{\mathrm{harv}} \leq \bar{h}_u \big(\tau - \sum_{v \in \mathcal{U}} \gamma_v\big), \forall u \in \mathcal{U}$. Moreover, energy feasibility implies

$$\gamma_u p^{\mathrm{up}} \leq e_u^{\mathrm{harv}}, \qquad \forall u \in \mathcal{U},$$

and the policy π limits the UE time to t_u, therefore $\gamma_u \leq t_u$. Hence every feasible solution of Problem 1 satisfies

$$0 \leq \gamma_u \leq t_u, \qquad \gamma_u p^{\mathrm{up}} \leq \bar{h}_u \left(\tau - \sum_{v \in \mathcal{U}} \gamma_v\right), \qquad \forall u \in \mathcal{U}.$$

Letting

$$T \triangleq \tau - \sum_{v \in \mathcal{U}} \gamma_v,$$

we obtain feasibility for (23)–(25). Therefore, every feasible solution of Problem 1 is feasible for the relaxed problem (22), and thus

$$J_{\rm ov}^{\star} \leq \sum_{u \in \mathcal{U}} \log\left(\frac{\hat{\gamma}_u c_u}{\tau}\right).$$

Subtracting

$$J_{\rm no}^{\star} = \sum_{u \in \mathcal{U}} \log\left(\frac{\gamma_u^{\rm DP} c_u}{\tau}\right) \tag{28}$$

proves (26). Non-negativity follows because the non-overlapping feasible set is a restriction of the unrestricted one. Finally, if (28) holds, the DP solution attains the upper bound, hence $J_{\rm no}^{\star} = J_{\rm ov}^{\star}$.

References

[1] J. Tang, D. K. So, A. Shojaeifard, K.-K. Wong, and J. Wen, "Joint antenna selection and spatial switching for energy efficient mimo swipt system," *IEEE Transactions on Wireless Communications*, vol. 16, no. 7, pp. 4754–4769, 2017.

[2] H. Shi, H. Ju, Y. Long, and W. Wang, "Can swipt-based mec system benefit from mmwave band: A joint beam, task offloading and energy harvesting optimization perspective," *IEEE Transactions on Vehicular Technology*, p. 1–10, 2024.

[3] Y. Zhang and C. You, "Swipt in mixed near- and far-field channels: Joint beam scheduling and power allocation," *IEEE Journal on Selected Areas in Communications*, vol. 42, no. 6, pp. 1583–1597, 2024.

[4] S. Zargari, A. Hakimi, C. Tellambura, and S. Herath, "User scheduling and trajectory optimization for energy-efficient irs-uav networks with swipt," *IEEE Transactions on Vehicular Technology*, vol. 72, no. 2, pp. 1815–1830, 2022.

[5] Y. Li, Y. Wu, Y. Song, L. Qian, and W. Jia, "Dynamic user-scheduling and power allocation for swipt aided federated learning: A deep learning approach," *IEEE Transactions on Mobile Computing*, vol. 22, no. 12, pp. 6956–6969, 2022.

[6] G. Rizzo, M. A. Marsan, C. Esposito, and B. Boi, "Green operations of swipt networks: The role of end-user devices," *IEEE Transactions on Green Communications and Networking*, 2025.

[7] Z. Wang, J. He, X. Liang, and L. Ge, "A novel swipt channel model and jointly age optimization in swipt-enabled access networks based on age of energy harvesting," *Scientific Reports*, vol. 15, no. 1, p. 10377, 2025.

[8] W. Lee, K. Lee, H.-H. Choi, and V. C. Leung, "Deep learning for swipt: Optimization of transmit-harvest-respond in wireless-powered interference channel," *IEEE Transactions on Wireless Communications*, vol. 20, no. 8, pp. 5018–5033, 2021.

[9] Y. Gao, Q. Wu, G. Zhang, W. Chen, D. W. K. Ng, and M. Di Renzo, "Beamforming optimization for active intelligent reflecting surface-aided swipt," *IEEE Transactions on Wireless Communications*, vol. 22, no. 1, pp. 362–378, 2022.

[10] Q. Shi, L. Liu, W. Xu, and R. Zhang, "Joint transmit beamforming and receive power splitting for miso swipt systems," *IEEE Transactions on Wireless Communications*, vol. 13, no. 6, pp. 3269–3280, 2014.

[11] J. Wildman, P. H. J. Nardelli, M. Latva-aho, and S. Weber, "On the joint impact of beamwidth and orientation error on throughput in directional wireless poisson networks," *IEEE Transactions on Wireless Communications*, vol. 13, no. 12, pp. 7072–7085, 2014.

[12] E. Boshkovska, D. W. K. Ng, N. Zlatanov, and R. Schober, "Practical non-linear energy harvesting model and resource allocation for swipt systems," *IEEE Communications Letters*, vol. 19, no. 12, pp. 2082–2085, 2015.